

Supernumerary Robotic Limbs for Next Generation Space Suit Technology

Erik Ballesteros¹, Brandon Man², H. Harry Asada³, *Fellow, IEEE*

Abstract—This paper discusses the incorporation of a pair of Supernumerary Robotic Limbs (SuperLimbs) onto the next generation of NASA space suits. The wearable robots attached to the space suit assist an astronaut in performing Extra-Vehicular Activities (EVAs). The SuperLimbs grab handrails fixed to the outside of a space vehicle to securely hold the astronaut body. The astronaut can use both hands for performing an EVA task, rather than using one hand for securing the body or operating a tether. The SuperLimbs can also assist an astronaut in repositioning the body and stabilizing it during an EVA mission. A control algorithm based on Admittance Control is developed for a) virtually reducing the inertial load of the entire body so that an astronaut can reposition his/her body with reduced effort, and b) bracing the body stably despite reaction forces and disturbances acting on the astronaut during an EVA operation. A full-scale prototype of Space Suit SuperLimbs was constructed and tested. Results from the experimentation indicated that with the aid of SuperLimbs, energy consumption during EVAs is reduced significantly.

Index Terms—Supernumerary Robotic Limbs, Wearable Robotics, Human-Assistive Robotics, Human-Robot Interaction, Spacesuits, Astronaut Ergonomics, Static Bracing, Admittance Control

I. INTRODUCTION

Extra-Vehicular Activities (EVAs) are a necessary and complex operation undertaken during any spaceflight mission. Astronauts place themselves within an extreme environment and must work within a pressurized space suit to complete often difficult tasks [1]. Despite extensive efforts at NASA, it has been a challenge to fully mitigate the risks associated with EVAs, reduce the workload of astronauts, and improve productivity. In general, astronauts carry around a foot-restraint which they rigidly fixate to a spacecraft's external structure to gain use of both arms, but severely limits their available work envelope [2]. Alternatively, the use of the Space Station Remote Manipulator System (SSRMS) can be used to manipulate the astronaut's position over a worksite, but is often cumbersome and introduces significant reliability and safety risks [3]. This paper proposes the use of a robotic system attached to the space suit of an astronaut for improving the ergonomics and capabilities of astronauts during EVA operations.

Supernumerary Robotic Limbs, or SuperLimbs for short, are a type of wearable robots attached to the body of a human [4], [5], [6]. We propose to incorporate SuperLimbs into a space

¹Erik Ballesteros is with the Department of Mechanical Engineering at the Massachusetts Institute of Technology balleste@mit.edu

²Brandon Man is with the Department of Computer Science at Cornell University

³H. Harry Asada is with the Department of Mechanical Engineering at the Massachusetts Institute of Technology asada@mit.edu

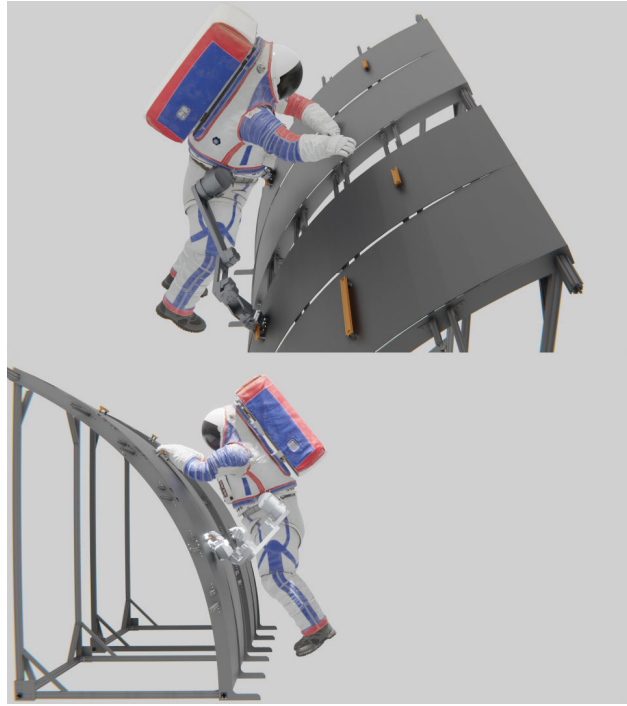


Fig. 1. Space Suit SuperLimbs System Concept.

suit so that an astronaut can possess additional appendages, such as a third arm and a fourth leg.

These SuperLimbs work in coordination with the astronaut as a portable rigid tether as well as a collaborative assistant in various EVA operations. For astronauts working on the ground for planetary explorations, the SuperLimbs can provide them with standing/lifting support, fall protection, incapacitated rescue operations, etc. For the initial development of this system, we look at EVAs conducted in micro-gravity environments, like that of the International Space Station (ISS). SuperLimbs attached to a space suit will allow the astronaut to move across the outside of the spacecraft, reposition the body, and secure it against a handrail or other fixtures on the spacecraft. The astronauts can use both hands for executing a mission task, rather than using one hand or both to secure the body. This would improve the productivity of EVA operations and reduce the astronaut workload and, thereby, reduce energy consumption.

Prior work on SuperLimbs has levitated towards applications in supporting a human operator subjected to gravitational effects, such as personnel in the construction and agricul-

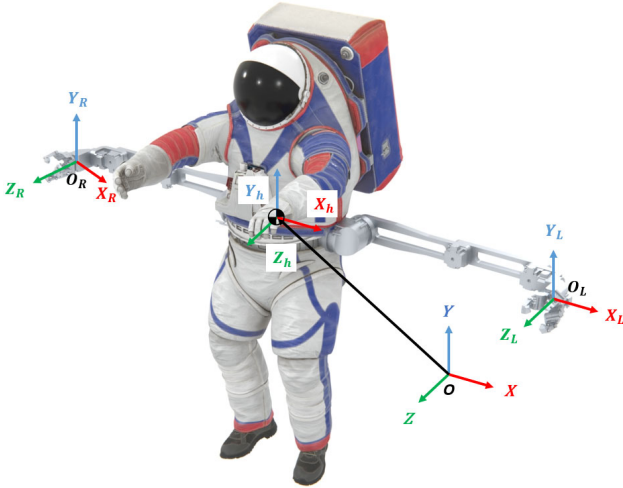


Fig. 2. Space Suit SuperLimbs System Coordinate Frames.

tural industries for improved worksite ergonomics [5], [7], [8]. These applications focus primarily on static posturing, where impedance and position control policies are enforced. However, working conditions in micro-gravity environments require the use of SuperLimbs to provide effective bracing that can be maintained while the user is in motion with minimal oversight [9]. A control policy, such as admittance control, has been shown to be an effective user interface when the operator is required to perform manipulation tasks [10], [11].

In the following discussion, a novel design concept of SuperLimbs incorporated into a space suit will be presented. A control algorithm, based on admittance control [12], [13], will be developed for assisting an astronaut in repositioning the body and securing the body despite disturbing loads. To validate the proposed design and control method, we developed a full-scale functional prototype of the Space Suit SuperLimbs system with a suspended testing environment to simulate micro-gravity EVA operations. With this prototype, we incorporated the Admittance Control Synthesis Scheme (ACSS), and evaluated the claims made in this discussion.

II. DESIGN CONCEPT

Fig. 1 shows a schematic of Space Suit SuperLimbs attached to a space suit. A pair of robot arms are placed around the waist and secured to the base frame of the space suit [14]. Each SuperLimb has a gripper that can securely grab a handrail [9] or other fixtures outside a space vehicle.

Two SuperLimbs are used for:

- Securely bracing the astronaut body and the space suit; a single SuperLimb forms merely an open-kinematic chain, which is limited in structural strength and load bearing capacity.
- Securely moving across the outside surface of a space vehicle, so that at least one SuperLimb is at all times grabbing a handrail including transitions from one handrail to another.

Each SuperLimb has a 6-axis force-torque sensor embedded in its end-effector, or at the wrist joint where a gripper is mounted. The two wrist force sensors measure the force and moment acting between the SuperLimbs and the handrail fixtures being grabbed by the SuperLimbs. As the astronaut performs an EVA task, he/she interacts with the space vehicle's exterior structure. These interactions can be monitored with the two 6-axis wrist force sensors. The Space Suit SuperLimbs can assist an astronaut in many ways. Specifically, the current work addresses the following two major functions for micro-gravity EVAs.

Tethering and bracing anywhere When an astronaut is positioned over a worksite, the SuperLimbs allows the astronaut to use both hands for executing a task and does so at a posture that is ergonomically effective and comfortable for the astronaut. Current state-of-the-art practices employ the use of a foot-restraint that can be installed at predetermined mounting locations on the external structure of the ISS or at the end-effector of the SSRMS. This practice results in mission planners having to meticulously design a task to be within an astronaut's work envelope to mitigate work postures susceptible to high safety risks [15]. In other cases, these foot-restraints cannot be used, and the astronauts must statically brace themselves with one of their arms [16]. A pair of SuperLimbs provide the astronaut with a fully rigid and adjustable tether anywhere during an EVA. This allows not only mission planners more flexibility in task design for EVAs, but it also allows astronauts to define their own comfortable worksite posture for a given task.

Inertial Mass Reduction During a micro-gravity EVA, astronauts must transfer themselves from one location to another in order to reach target worksites or the airlock. These transfer operations are conducted primarily by the astronaut applying a load to an external structure to generate propulsion. The astronaut must push or pull the entire inertia of his/her body and the space suit. In case the astronaut must reposition his/her body frequently it may be more energy consuming. Furthermore, in case of emergencies and instances where a quicker transfer is required, astronauts run the risk of creating high joint torques which consequentially results in high energy exertion that presents a significant safety risk [1], [17].

With a pair of SuperLimbs assisting the astronaut's movements, the SuperLimbs can virtually reduce the overall effective inertia of the astronaut and space suit, as to be later discussed. This enables the astronaut to exert smaller joint torques to achieve higher velocity transfers, thus mitigating high energetic consumption.

III. CONTROL

A. Modeling

Coordinate systems are defined in Fig. 2. Frame $O - XYZ$ is the Inertial Reference Frame, $O_R - X_R Y_R Z_R$ and $O_L - X_L Y_L Z_L$ are frames attached to the end-effectors of the right and left SuperLimbs, respectively. Let $\dot{P}_h \in R^6$ be velocity and angular velocity at the Center of Mass (CoM) of the

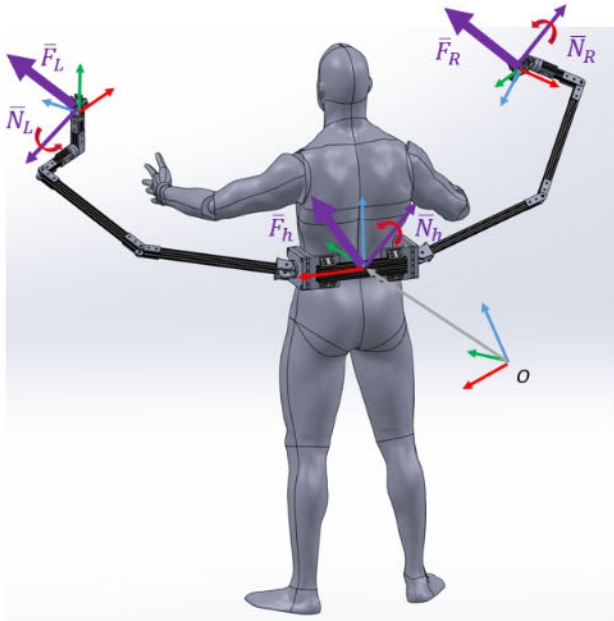


Fig. 3. External Forces/Moments applied to Space Suit SuperLimbs System

human, while $\dot{P}_R, \dot{P}_L \in R^6$ be, respectively, those of the right and left end-effectors. We have

$$\begin{aligned}\dot{P}_R &= J_R \dot{q}_R + \dot{P}_h \\ \dot{P}_L &= J_L \dot{q}_L + \dot{P}_h\end{aligned}\quad (1)$$

where $\dot{q}_R, \dot{q}_L \in R^6$ are joint velocities and $J_R, J_L \in R^{6 \times 6}$ are the Jacobians of the right and left SuperLimbs, respectively. Suppose that the SuperLimbs are securely holding handrails on some structure of a spacecraft, $\dot{P}_R = \dot{P}_L = 0$. Then,

$$\therefore \dot{P}_h = -J_R \dot{q}_R = -J_L \dot{q}_L \quad (2)$$

Assuming that the entire astronaut's body, including the space suit and the Personal Protective Equipment (PPE), as a single body of total mass m_h and moment of inertia I_h , we obtain the equation of motion given by

$$\begin{aligned}m_h \ddot{X}_h &= \bar{\mathbf{F}}_h \\ I_h \dot{\omega}_h + \omega_h \times (I \omega_h) &= \bar{\mathbf{N}}_h\end{aligned}\quad (3)$$

where $\bar{\mathbf{F}}_h$ and $\bar{\mathbf{N}}_h$ are force and moment, or collectively a wrench, acting at the human CoM. Vectors \dot{X}_h and ω_h are linear and angular velocities of \dot{P}_h , called a twist.

$$\mathbf{F}_h = \begin{bmatrix} \bar{\mathbf{F}}_h \\ \bar{\mathbf{N}}_h \end{bmatrix}, \dot{P}_h = \begin{bmatrix} \dot{X}_h \\ \omega_h \end{bmatrix} \quad (4)$$

It can be assumed that ω_h is small enough to ignore $\omega_h \times (I_h \omega_h)$, the above equation of motion can be reduced to

$$M \ddot{P}_h = \mathbf{F}_h \quad (5)$$

$$\text{where } M = \begin{bmatrix} m_h I_3 & 0 \\ 0 & I_h \end{bmatrix} \quad (6)$$

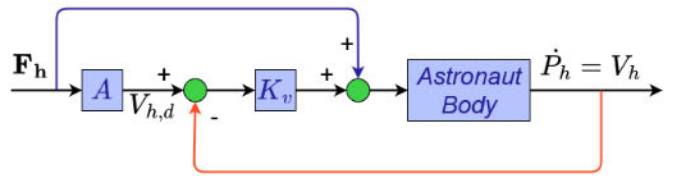


Fig. 4. Admittance Control Synthesis Block Diagram for Space Suit SuperLimbs System.

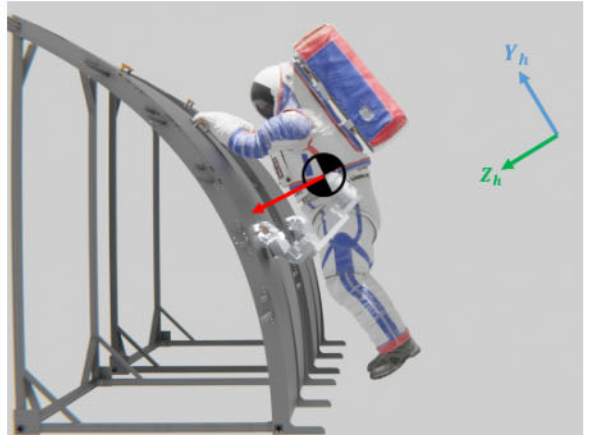


Fig. 5. Proximity of astronaut to ISS external structure.

B. Admittance Control

An astronaut must be able to change his/her position when performing EVA operations. Despite the significant inertia of the entire body M , the astronaut pushes/pulls the whole body by grabbing handrails on the exterior of the ISS for re-positioning the body. The SuperLimbs can assist the astronaut by virtually reducing the body inertia. Also, the SuperLimbs can brace the body to maintain the current position and orientation of the body. Furthermore, the SuperLimbs can bear a disturbing load acting on the body. Performing drilling work, for example, the astronaut must brace his/her body to absorb the disturbances generated by the hand-drill. Here, we consider the two functions of the SuperLimbs.

- 1) Virtually reduce the body inertia for agile and power-effective maneuvering.
- 2) Disturbance rejection by bracing the body.

Both functions required for the Space Suit SuperLimbs can be realized by controlling a functional relation between the wrench acting on the astronaut \mathbf{F}_h and the resultant velocity of the body.

Consider the following admittance control law.

$$V_{h,d} = A \mathbf{F}_h \quad (7)$$

where $A \in R^{6 \times 6}$ is an admittance matrix relating the body velocity to the wrench acting on the body. Fig. 4 shows the block diagram of the admittance control system. A velocity feedback control loop is formed from the actual astronaut's body velocity and angular velocity \dot{P}_h with a velocity feedback

gain matrix $K_v \in R^{6 \times 6}$. The wrench \mathbf{F}_h directly acts on the astronaut's body through the feedforward path at the top of the block diagram. The resultant wrench $\mathbf{F}_h + K_v(\dot{P}_{h,d} - \dot{P}_h)$ acts on the astronaut's body. The admittance control system measures the wrench \mathbf{F}_h and computes the desired velocity $\dot{P}_{h,d}$ in response to \mathbf{F}_h , as stipulated by the admittance control law (7). The wrench \mathbf{F}_h includes the force generated by the astronaut; when re-positioning, the astronaut pushes/pulls handrails, for example. The wrench \mathbf{F}_h also includes a disturbance force generated during an EVA operation.

From the diagram and the equation of motion (5), we obtain

$$M\ddot{P}_h = \mathbf{F}_h + K_v(A\mathbf{F}_h - \dot{P}_h) \quad (8)$$

Taking the Laplace transform, we obtain

$$V_h = [K_v^{-1}Ms + I]^{-1}[A + K_v^{-1}]\mathbf{F}_h \quad (9)$$

where $V_h = \dot{P}_h$ and K_v is assumed non-singular. As the velocity gain matrix is sufficiently high, the above relationship reduces to

$$V_h \cong A\mathbf{F}_h \quad (10)$$

which is approximately the same as (7). For a finite K_v , note that the inertia felt by the astronaut virtually reduces to $K_v^{-1}M$ in (9). This is to meet the first functional requirement described above.

The admittance matrix A in (7) and (10) represents the inverse of a damping matrix. With a larger A , the damping virtually reduces, and the response becomes more agile. The two gain matrices, K_v and A , allow us to tune the behavior of the Space Suit SuperLimbs to desired dynamics.

As for the second functional requirement, the disturbance acting on the astronaut, \mathbf{F}_h , can be attenuated by assigning the admittance matrix A to

$$A = -\eta K_v^{-1} \quad (11)$$

where η is a parameter, $0 \leq \eta \leq 1$. Substituting this into (9) yields

$$V_h = [K_v^{-1}Ms + I]^{-1}(1 - \eta)\mathbf{F}_h \quad (12)$$

Setting $\eta = 1$ completely rejects the disturbances. This admittance control entails the measurement of the wrench \mathbf{F}_h acting on the astronaut. As described previously, both SuperLimbs are equipped with 6 axis wrist force sensors measuring the wrench acting on the individual end-effectors. The wrench \mathbf{F}_h can be estimated based on the two wrist force sensor measurements and the state of the astronaut motion. A Kalman Filter, for example, can be used for estimating $\hat{\mathbf{F}}_h$. In the current work, however, a simple method is used for estimating $\hat{\mathbf{F}}_h$ by assuming that $M\ddot{P}_h$ is small.

$$\hat{\mathbf{F}}_h = -S_R\mathbf{F}_R^R - S_L\mathbf{F}_L^L \quad (13)$$

where \mathbf{F}_R^R and \mathbf{F}_L^L are 6-axis force sensor readings at the right and left end-effectors in their coordinate frames, respectively,

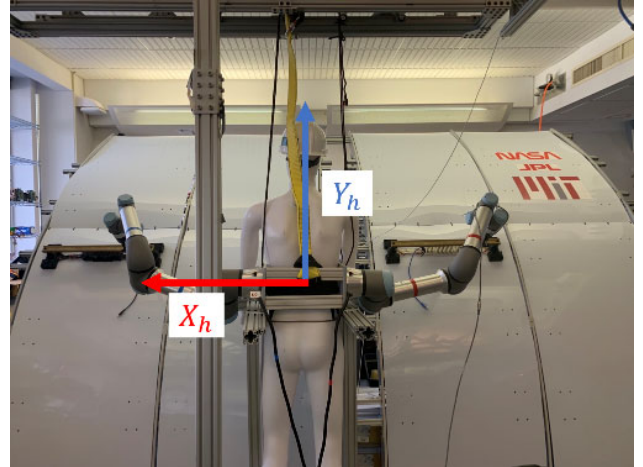


Fig. 6. Space Suit SuperLimbs functional ground testing apparatus.

and S_R and S_L are transformation matrices between the end-effector frames and the human frame given by

$$S_i = \begin{bmatrix} I & 0 \\ s_i & I \end{bmatrix} \quad s_i = \begin{bmatrix} 0 & -r_{zi} & r_{yi} \\ r_{zi} & 0 & -r_{xi} \\ -r_{yi} & r_{xi} & 0 \end{bmatrix} \quad (14)$$

where (r_x, r_y, r_z) are coordinates of each end-effector viewed from the human frame.

IV. DESIGN AND IMPLEMENTATION

We utilized two Universal Robots UR5e robots, which were connected to an extruded aluminum frame with a human mannequin rigidly installed, as shown in Fig. 6. This entire prototype is suspended overhead by an enclosed rail capable of translating +/- 0.5 m in the X inertial axis to simulate a partial micro-gravity environment (along the X and Z inertial axes with consideration provided to restoring equilibrium forces due to gravity). To simulate the external structure, a full-scale sectional mock-up of the exterior of the ISS was developed, with the capability of having instrumented EVA handrails installed at a variety of different locations.

The ACSS was developed in a Python script that communicates with two UR5e robots via ROS2 Foxy (and Real-Time Data Exchange (RTDE) as a redundancy). The UR5e's onboard F/T sensor data as well as the joint state data of each robot was acquired by directly subscribing to each telemetry topic and recording that data into a rosbag file at a stable sampling rate of 100 Hz, which was then converted into a .csv file for data synthesis.

Outside of the robot instrumentation, to measure the external loads applied by the test operator, a plate with an inline HX711 load cell will be pushed by the test operator and recorded separately at a stable sampling rate of 10 Hz.

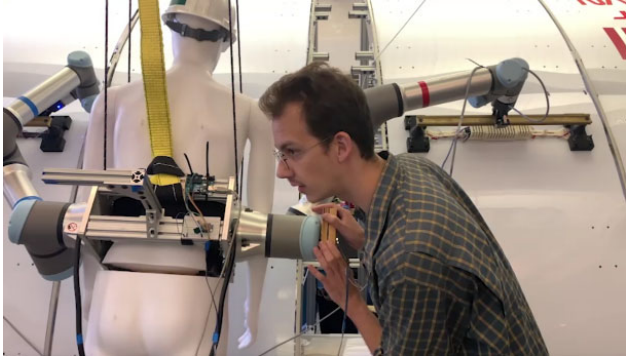


Fig. 7. Push Test on Space Suit SuperLimbs prototype.

V. EXPERIMENTATION

A. Experimental Setup

In order to validate the Space Suit SuperLimbs system, two distinct experiments (and one simulation analysis) were performed on the prototype to validate both the Space Suit SuperLimbs' performance in statically bracing the astronaut as well as the physical implementation of the ACSS (with regard to its effectiveness in attenuating the effective inertial mass of the astronaut).

- 1) To assess the static bracing performance, a compliance controller [18] was implemented onto the prototype with varying virtual stiffness, K , at a constant applied load of 89 N (20 lbf) in the $+/-X_h$, $+/-Y_h$, and $+/-Z_h$ directions for approximately 3 seconds, shown in Fig. 7. For each test, the total deflection of one of the robot's end-effector position was recorded.
- 2) To evaluate the attenuation in effective inertial mass, a low applied force (approximately 10 N) was applied in the $+/-X_h$ directions for each proportional gain setting, K_v , shown in Table I (with *Free Floating* referring to no SuperLimb connection with the structure, test operator is purely pushing the mass of the prototype). With each test the power, work, and time required for the test operator to successfully traverse the mannequin's CoM 0.33 m was determined. In this experimental setup, we considered that the tasks the astronaut would need to perform can be represented along the X_h axis.

For both of these experiments, additional testing would need to be performed in a higher fidelity environment for microgravity EVAs (such as NASA's Neutral Buoyancy Laboratory (NBL) or Active Response Gravity Offload System (ARGOS)) in order to reaffirm the design of this system in 6 DoF.

In addition to these two experiments, an analysis in MATLAB was performed to investigate the Space Suit SuperLimbs' capacity to provide the astronaut with positional adjustment over a worksite. To perform this analysis, the astronaut's CoM

TABLE I
ASTRONAUT PERFORMANCE WITH SPACE SUIT SUPERLIMBS

Gain K_v	Avg. P (W)	W_d (J)	$t_{0.33m}$ (s)
Free Floating	6.10	53.53	7.8
2	3.85	33.75	5.5
3	3.50	24.25	5.4
5	3.33	12.75	4.7
10	2.97	10.31	3.9
25	1.29	7.50	3.4

workspace due to the SuperLimbs must be determined. By assuming that the SuperLimbs' end-effectors are rigidly fixed to the external structure, we analyzed the work spaces of both SuperLimbs with respect to their end-effectors, and overlapped them to determine the workspace for an astronaut's CoM.

B. Results/Discussion

Fig. 8 plots the total deflection of the prototype's CoM with varying stiffness from the compliance controller. It should be noted that $K = \text{Max}$ refers to a completely stiff set of SuperLimbs.

Fig. 9 shows the power applied by the test operator over the time it takes to translate the prototype CoM 0.33 m from both a free floating configuration where the SuperLimbs are not rigidly fixated to any structure, and an active SuperLimb configuration (both end-effectors fixed to the structure) with a velocity feedback gain, K_v , of 5. For each test, the work applied by the test operator was calculated by integrating each power curve, fully tabulated in Table I.

During the execution of Experiment 2, the motion of the prototype's CoM was highly oscillatory in behavior with occasional unstable motion profiles that led to safeguards being activated by the URs and prematurely terminating tests. This was due to the fact that the force feedback of the experimental setup is non-collocated with a low sampling rate of 100 Hz [19]. A forward action is to optimize the prototype's controller for higher stable sampling rates to broaden the system's stability and repeat those tests with smoother motion profiles. Despite these hardware limitations, reasonable applied load data from the test operator was still captured and able to be disseminated for this study.

Fig. 10 illustrates the overlap of both SuperLimb work spaces when the astronaut's CoM is 0.66 m from the external structure. This shows that the astronaut's workspace can be characterized by an ellipse with a major axis of 1.6 m in the Y axis and a minor axis of 1.0 m in the X axis.

The Space Suit SuperLimbs show good static bracing performance, where the astronaut's CoM deflections are reduced and can be tuned. Likewise, the ACSS presents good performance in regards to reducing the overall effective inertial mass. The work required for an astronaut to propel their body is reduced with our admittance control design. Additionally, the working envelop of the astronaut can be expanded by

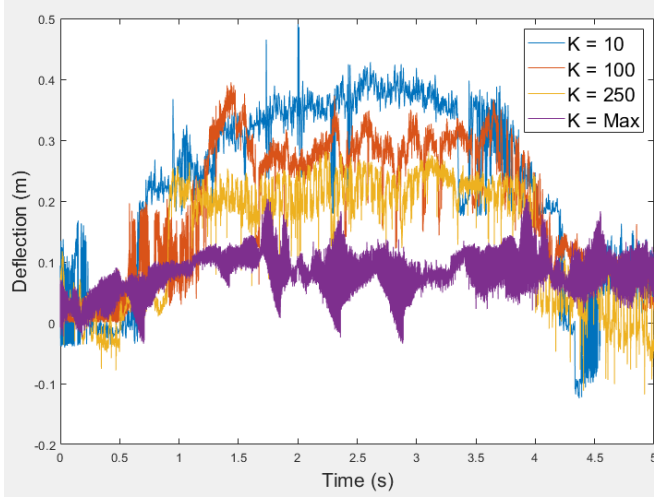


Fig. 8. Total deflection of astronaut CoM during a stationary hold operation.

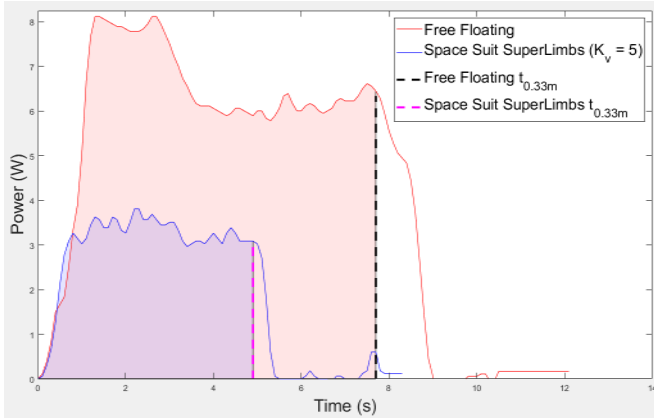


Fig. 9. Power required by astronaut to translate 0.33 m.

the workspace of the SuperLimbs. This demonstrates that SuperLimbs can effectively provide mitigation in energy consumption and offer a viable solution for bracing/tethering an astronaut's body, whether static or in motion.

VI. CONCLUSION

In this study, we devised a novel integration approach to the way EVAs are conducted by attaching a pair of SuperLimbs to a space suit. For the initial development of this effort, we analyzed how the Space Suit SuperLimbs system affects microgravity EVAs and discovered that the system can provide risk mitigation for astronaut safety and health by alleviating conditions in which the astronaut must apply high joint torques within the space suit. This is done so by attenuating the effective overall inertial mass gained by the admittance control design as well as providing a portable and adjustable rigid tether through a means of disturbance rejection, allowing the astronaut more flexibility in worksite posturing as well as expanding the work envelope for astronauts. Simulation and experimental results show that this integration approach does in fact meet these analytical findings.

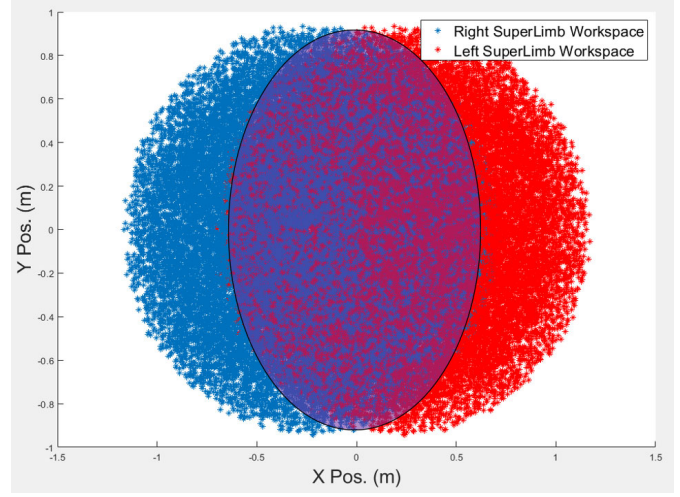


Fig. 10. Rigid Tether allowable movement profile of astronaut CoM with astronaut CoM 0.66 m from external structure (shown in purple).

Future work will need to be conducted in regards to validating the disturbance rejection of the Space Suit SuperLimbs system. This can be done by conducting additional experiments that evaluate the Space Suit SuperLimbs' response to loads induced during common EVA worksite tasks, like the use of a hand-drill, and loads induced when an astronaut is actively transferring from one worksite to another.

The studies and development conducted thus far for the Space Suit SuperLimbs demonstrates a promising solution for future NASA EVAs. Future development of the Space Suit SuperLimbs system will be done so to align with NASA's current technological interests in planetary EVAs [1]. This means that the concepts discussed above will be expanded to worksite tasks with a partial gravity environment. This enables a much broader assortment of unique applications of SuperLimbs that will yield in the future further academic discussion.

REFERENCES

- [1] A. Abercromby, B. Alpert, J. Cupples, E. Dillon, A. Garbino, Y. Hernandez, C. Kovich, M. Miller, J. Norcross, C. Pittman, S. Rajulu, and R. Rhodes, "Crew health and performance extravehicular activity roadmap: 2020," National Aeronautics and Space Administration, Tech. Rep., 2020.
- [2] *NASA Spaceflight Human-System Standard; Volume 2: Human Factors, Habitability, and Environmental Health*, National Aeronautics and Space Administration Std., Rev. 3, 2019.
- [3] M. Chang and J. Marquez, "Human-automation allocations for current robotic space operations: Space station remote manipulator system," National Aeronautics and Space Administration, Tech. Rep., 2018.
- [4] F. Parietti, K. Chan, and H. H. Asada, "Bracing the human body with supernumerary Robotic Limbs for physical assistance and load reduction," in *2014 IEEE International Conference on Robotics and Automation (ICRA)*. IEEE, 2014, pp. 141–148.
- [5] Y. Tong and J. Liu, "Review of Research and Development of Supernumerary Robotic Limbs," *IEEE/CAA Journal of Automatica Sinica*, vol. 8, no. 5, pp. 929–952, 2021.
- [6] J. Eden, M. Bräcklein, J. Ibáñez, D. Y. Barsakcioglu, G. Di Pino, D. Farina, E. Burdet, and C. Mehring, "Principles of human movement augmentation and the challenges in making it a reality," *Nature Communications*, vol. 13, no. 1, p. 1345, 2022.

- [7] D. A. Kurek and H. H. Asada, "The MantisBot: Design and impedance control of supernumerary robotic limbs for near-ground work," in *2017 IEEE International Conference on Robotics and Automation (ICRA)*. IEEE, 2017, pp. 5942–5947.
- [8] D. J. Gonzalez and H. H. Asada, "Design of Extra Robotic Legs for Augmenting Human Payload Capabilities by Exploiting Singularity and Torque Redistribution," in *2018 IEEE/RSJ International Conference on Intelligent Robots and Systems (IROS)*. IEEE, 2018, pp. 4348–4354.
- [9] D. R. Liskowsky and W. W. Seitz, *Human Integration Design Handbook (HIDH)*, 1st ed., National Aeronautics and Space Administration, 2014.
- [10] G. Gourmelen, A. Verhulst, B. Navarro, T. Sasaki, G. Gowrishankar, and M. Inami, "Co-Limbs: An Intuitive Collaborative Control for Wearable Robotic Arms," in *SIGGRAPH Asia 2019 Emerging Technologies*. ACM, 2019, pp. 9–10.
- [11] W. Kim, P. Balatti, E. Lamon, and A. Ajoudani, "MOCA-MAN: A MOBILE and reconfigurable Collaborative Robot Assistant for conjoined huMAN-robot actions," in *2020 IEEE International Conference on Robotics and Automation (ICRA)*. IEEE, 2020, pp. 10191–10197.
- [12] C. Ott and Y. Nakamura, "Admittance Control using a Base Force/Torque Sensor." *IFAC Proceedings Volumes*, vol. 42, no. 16, pp. 467–472, 2009.
- [13] A. Q. Keemink, H. van der Kooij, and A. H. Stienen, "Admittance control for physical human–robot interaction." *The International Journal of Robotics Research*, vol. 37, no. 11, pp. 1421–1444, 2018.
- [14] A. Ross, R. Rhodes, and S. McFarland, "Nasa's advanced extra-vehicular activity space suit pressure garment 2018 status and development plan," in *48th International Conference on Environmental Systems*. SAE International, 2018.
- [15] P. Schmidt, "An investigation of space suit mobility with applications to EVA operations," Ph.D. dissertation, Massachusetts Institute of Technology, 2001.
- [16] NASA. Spacewalk to install new international space station solar arrays. (Jun. 20, 2021) Accessed: Mar. 15, 2022. [Online Video]. Available: <https://www.youtube.com/watch?v=gCKsedpraVg>.
- [17] D. J. Newman, P. B. Schmidt, and D. B. Rahn, "Modeling the Extravehicular Mobility Unit (EMU) Space Suit: Physiological Implications for Extravehicular Activity (EVA)," in *30th International Conference on Environmental Systems*. SAE International, 2000.
- [18] D. Surdilovic, Y. Yakut, T.-M. Nguyen, X. B. Pham, A. Vick, and R. Martin-Martin, "Compliance control with dual-arm humanoid robots: Design, planning and programming," in *2010 10th IEEE-RAS International Conference on Humanoid Robots*. IEEE, 2010, pp. 275–281.
- [19] C. Veronneau, J. Denis, L.-P. Lebel, M. Denninger, J.-S. Plante, and A. Girard, "A Lightweight Force-Controllable Wearable Arm Based on Magnetorheological-Hydrostatic Actuators," in *2019 International Conference on Robotics and Automation (ICRA)*, vol. 2019. IEEE, 2019, pp. 4018–4024.